

# Control of spatiotemporal chaos by stochastic resetting

Camille Aron<sup>1,2,\*</sup> and Manas Kulkarni<sup>3,†</sup>

<sup>1</sup>*Institute of Physics, École Polytechnique Fédérale de Lausanne (EPFL), CH-1015 Lausanne, Switzerland*

<sup>2</sup>*Laboratoire de Physique de l'École Normale Supérieure, ENS, Université PSL, CNRS, Sorbonne Université, Université Paris Cité, F-75005 Paris, France*

<sup>3</sup>*International Centre for Theoretical Sciences, Tata Institute of Fundamental Research, Bangalore 560089, India*  
(Dated: December 31, 2024)

We study how spatiotemporal chaos in dynamical systems can be controlled by stochastically returning them to their initial conditions. Focusing on discrete nonlinear maps, we analyze how key measures of chaos—the Lyapunov exponent and butterfly velocity, which quantify sensitivity to initial perturbations and the ballistic spread of information, respectively—are reduced by stochastic resetting. We identify a critical resetting rate that induces a dynamical phase transition, characterized by the simultaneous vanishing of the Lyapunov exponent and butterfly velocity, effectively arresting the spread of information. These theoretical predictions are validated and illustrated with numerical simulations of the celebrated logistic map and its lattice extension. Beyond discrete maps, our findings offer insights applicable to a broad class of extended classical interacting systems.

*Introduction.*— The spatiotemporal scrambling of information in chaotic many-body systems [1–5] not only underpins the foundations of statistical physics but also poses substantial practical challenges for the smooth operation of information processing devices as their complexity increases [6]. Throughout the history of classical computing, various strategies have been developed to address these challenges and ensure reliable operation within regular dynamical regimes. These include approaches based on feedback and optimal control [7], advanced techniques in control theory [8], stabilizing periodic orbits via probabilistic control [9–11], and the imposition of dynamical constraints [12, 13]. Although this subject has been extensively studied across diverse communities, out-of-time-order correlations (OTOCs) have recently emerged as a relatively transparent probe of spatiotemporal chaos. They bring the well-developed toolbox of correlation functions to the study of dynamical systems. Initially introduced for quantum mechanical systems in the semiclassical regime [1–3, 14], OTOCs were subsequently studied in fully quantum systems, such as spin-1/2 chains [15, 16], and more recently applied to purely classical systems [17–26]. OTOCs quantify the temporal growth and spatial spread of perturbations between two copies of a system prepared with slightly different initial conditions. In classical systems, the exponential sensitivity to initial conditions—a hallmark of chaos—is characterized by Lyapunov exponents, while the ballistic propagation of information is captured by the light-cone structure of OTOCs and quantified by the butterfly velocity. Alongside ongoing efforts to understand the emergence of these two quantities in diverse classical or quantum setups, notably the influence of disorder [27–31], there is a growing interest in devising strategies to control them through externally engineered protocols.

In this work, we explore how stochastic resetting [32–36] can be harnessed to delay or suppress the onset of spatiotemporal chaos in classical interacting many-body systems. At its core, stochastic resetting consists in returning the state of a dynamical system to its initial condition at random times. Variations on this protocol include non-Poissonian resetting times, resetting to a cloud of initial conditions, and more. By and large, stochastic resetting has proven to be a versatile nonequilibrium protocol applicable to virtually any dynamical system, with relatively low analytical or computational overhead. It has also been demonstrated experimentally [37–39].

By introducing a new timescale, stochastic resetting can reshape the system’s transient and steady-state dynamics. In the context of random search problems, it can be used to dramatically reduce the mean first-passage time [40, 41]. From a thermodynamic perspective, stochastic resetting has been articulated within the framework of stochastic thermodynamics [42, 43]. However, much remains to be understood about the impact of stochastic resetting on the dynamics of extended interacting systems [44]. Studies have begun to explore the effects of resetting on correlations and dynamical phase transitions such as phase synchronization in the Kuramoto model [45–48], Kardar-Parisi-Zhang equation [49], exclusion process [50–52] and the Ising model [53, 54]. Conversely, stochastic resetting can serve as a resource for dynamically generating correlations between non-interacting particles or fields [55–57].

We question the fate of chaotic properties in interacting many-body dynamics subject to stochastic resetting, within the framework of discrete maps commonly used in the study of dynamical systems [58–60]. After formulating the discrete-time dynamics subject to stochastic resetting, we first focus on Lyapunov growth by analyzing zero-dimensional nonlinear maps subject to resetting. Subsequently, we study the spatiotemporal spread of information in extended systems, particularly the butterfly velocity, using coupled map lattices.

\* aron@ens.fr

† manas.kulkarni@icts.res.in

*Discrete-time maps under stochastic resetting.*— Let us consider the dynamics generated by a deterministic discrete-time map interspersed with random resetting events. The resulting stochastic map can be formulated as

$$x_n \mapsto x_{n+1} = \begin{cases} f(x_n) & \text{with probability } 1 - r \\ x_0 & \text{with probability } r, \end{cases} \quad (1)$$

for  $n \geq 0$ . Here,  $0 \leq r \leq 1$  is the rate at which trajectories are reset to their initial condition  $x_0$ . The state of the system at time  $n$  is given by  $x_n$ . Let us first examine how resetting affects the temporal aspect of chaos by considering zero-dimensional maps where  $f(x)$  is a non-linear function of  $x$ . Later, we shall examine the spatial aspects by generalizing to multidimensional-vector states living on a lattice of size  $L$ ,  $x_n = \{x_{n,i}\}_{i=1\dots L}$ . The dynamics in Eq. (1) are explicitly Markovian but this encompasses non-Markovian evolutions with finite time kernel at the cost of adding auxiliary degrees of freedom.

In the absence of resetting ( $r = 0$ ), the deterministic map  $f$  is assumed to be ergodic, reaching a unique stationary distribution  $p_{\text{st}}(x) := \lim_{N \rightarrow \infty} \frac{1}{N+1} \sum_{n=0}^N \delta(x - x_n) > 0 \forall x$ , independently of the choice of initial condition. Additionally, we assume that the deterministic map is chaotic. This manifests as a positive Lyapunov exponent  $\lambda$  defined as  $\lambda := \lim_{n \rightarrow \infty} \frac{1}{n} \log |\delta x_n / \delta x_0|$ , where  $\delta x_n$  is the variation of  $x_n$  due to an infinitesimal perturbation  $\delta x_0$  applied to the initial condition  $x_0$ . Ergodicity ensures that  $\lambda$  is independent of the choice of  $x_0$ .

In the presence of resetting ( $r > 0$ ), the dynamics in Eq. (1) generate stochastic trajectories. The corresponding ensemble average consists in sampling over the many possible realizations of the resetting times. We find that the stationary distribution is given by [61]

$$\tilde{p}_{\text{st}}(x) = \sum_{n=0}^{\infty} \tilde{g}_n \delta(x - x_n), \quad (2)$$

with  $\tilde{g}_n := r(1-r)^n \Phi(1-r, 1, 1+n)$  where  $\Phi$  is the Hurwitz–Lerch transcendent. Although  $\tilde{p}_{\text{st}}(x)$  depends on the choice of initial condition  $x_0$ , none of the results presented below depend on  $x_0$  and we do not perform any average over  $x_0$ . A rigorous assessment of the ergodicity of the resetting dynamics is challenging and, to the best of our knowledge, has not yet been addressed in the literature. On this specific matter, we shall make informed conjectures rather than definitive conclusions. To assess its chaotic behavior, *i.e.*, its sensitivity to perturbations of initial conditions, we define the Lyapunov exponent  $\tilde{\lambda}$  as

$$\tilde{\lambda} := \lim_{n \rightarrow \infty} \frac{1}{n} \log \left\langle \left| \frac{\delta x_n}{\delta x_0} \right| \right\rangle_r. \quad (3)$$

where  $\langle \dots \rangle_r$  denotes the average over resetting times. Unlike the deterministic case, the independence of  $\tilde{\lambda}$  with respect to  $x_0$  is nontrivial and will be clarified below.

The computation of  $\tilde{\lambda}$  is greatly simplified by expressing  $\tilde{d}_n := \langle |\delta x_n / \delta x_0| \rangle_r$  in Eq. (3) in terms of its deterministic counterpart:  $d_n := |\delta x_n / \delta x_0|$ . This is achieved by the renewal formula

$$\tilde{d}_n = \sum_{m=0}^{n-1} r(1-r)^m d_m + (1-r)^n d_n, \quad (4)$$

for  $n \geq 1$ , together with  $\tilde{d}_0 = d_0 = 1$ . Here, the summation on  $m$  accounts for averaging over the time elapsed since the last resetting event.

To simplify our analysis, we assume that the deterministic dynamics are characterized by a Lyapunov exponent  $\lambda$  of order 1 or greater. This implies that the exponential sensitivity to initial conditions,  $|\delta x_n / \delta x_0| \propto \exp(\lambda n)$ , develops as early as  $n = 1$  and we can neglect the sub-exponential contributions. With this chaotic ansatz in Eq. (4), resetting is found to renormalize the Lyapunov exponent according to

$$\tilde{\lambda} = \begin{cases} \lambda + \log(1-r) & \text{if } r < r_c \\ 0 & \text{if } r \geq r_c, \end{cases} \quad (5)$$

where  $r_c := 1 - e^{-\lambda}$ . This monotonous decay of the Lyapunov with  $r$  indicates that increasing the resetting probability systematically reduces the chaoticity of the dynamics. From Eq. (5), it is now clear that  $\tilde{\lambda}$  is independent of the initial condition  $x_0$ .  $\tilde{\lambda}$  vanishes at a critical resetting rate,  $r_c < 1$ , signaling a transition from chaotic to non-chaotic dynamics. For  $0 < r < r_c$ , the dynamics retain exponential sensitivity to initial conditions, and there remains a finite probability for trajectories to explore the entire phase space, preserving ergodicity. As  $r$  approaches  $r_c$ , the Lyapunov vanishes linearly:  $\tilde{\lambda} \propto (r - r_c)^\mu$  with the dynamical exponent  $\mu = 1$ . At  $r = r_c$ , a dynamical transition takes place: the exponential sensitivity to initial conditions is lost, and the system shifts to non-chaotic behavior. For  $r \geq r_c$ , the dynamics become non-chaotic and we present arguments in the Supplementary Material [61] indicating a concomitant loss of ergodicity. In this regime, trajectories consistently remain localized near their initial conditions, failing to escape their vicinity.

To numerically test the prediction in Eq. (5), we first reformulate the expression of the Lyapunov exponent in Eq. (3) using the relationship  $|\delta x_n / \delta x_0| = \prod_{p=0}^{n-1} |f'(x_p)|$  for  $n \geq 1$ . We obtain the explicit expression

$$\tilde{\lambda} = \lim_{n \rightarrow \infty} \frac{1}{n} \log \left[ r + r \sum_{m=1}^{n-1} (1-r)^m \prod_{p=0}^{m-1} |f'(x_p)| + (1-r)^n \prod_{p=0}^{n-1} |f'(x_p)| \right]. \quad (6)$$

This approach only requires analyzing a single trajectory of the non-resetting dynamics, thereby avoiding the complex calculations of linear responses to infinitesimal perturbations and the averaging over numerous resetting trajectories.

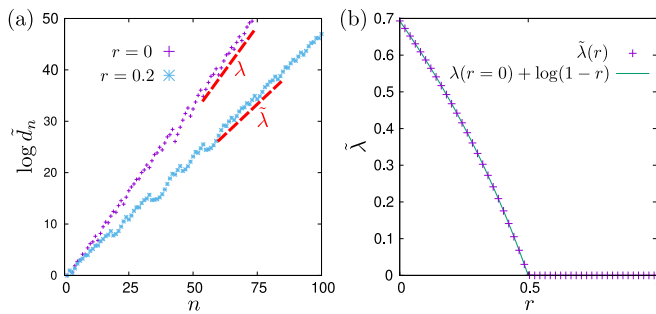


FIG. 1. Logistic map [Eq. (7),  $\alpha = 4$ ] subject to stochastic resetting. (a) Exponential sensitivity to initial perturbations for the deterministic map ( $r = 0$ ) and for a finite resetting rate ( $r = 0.2$ ). The former validates the exponential ansatz  $\log|\delta x_n/\delta x_0| \propto \lambda n$ , even at early times. The Lyapunov exponents  $\lambda = \log 2$  and  $\tilde{\lambda}$  can be extracted from the slopes. (b) The renormalized Lyapunov  $\tilde{\lambda}$  computed with Eq. (6) is compared to the analytical predictions of Eq. (5) as a function of the resetting rate  $r$ . The critical resetting is located at  $r_c = 1/2$ .

In practice, we work out the example of the celebrated logistic map which is an archetypal illustration of the onset of chaos [62–65]. It is defined as

$$f(x) = \alpha x(1 - x), \quad (7)$$

with  $x_0 \in [0, 1]$  and  $\alpha \in [0, 4]$  to ensure the stability of the interval  $x \in [0, 1]$  under the map. Let us note that the bifurcation diagram of the logistic map when varying  $\alpha \in [0, 4]$  remains invariant under stochastic resetting, provided an additional average is performed over initial conditions drawn from the stationary distribution of the deterministic map [61]. In practice, we work at  $\alpha = 4$  where the map exhibits fully developed chaos with a Lyapunov  $\lambda = \log 2$  and an ergodic stationary distribution given by  $p_{\text{st}}(x) = 1/(\pi\sqrt{x(1-x)})$  [66]. The results are shown in Fig. 1. The panel (a) validates the ansatz  $d_n \propto \exp(\lambda n)$  that was used to derive the renormalized Lyapunov  $\tilde{\lambda}$  in Eq. (5). In the panel (b), we directly compare these analytical predictions to the numerical results, where Lyapunov exponents are computed using Eq. (6). The agreement is excellent.

*Coupled map lattices (CML).*— We now examine the spatial aspect of chaos in the presence of stochastic resetting by considering discrete maps on lattices, commonly referred to as coupled map lattices [67–69]. For simplicity, we consider one-dimensional lattices of  $L$  sites with periodic boundary conditions. The state of the system at time  $n$  is now represented by a vector  $x_n$  with components  $x_{n,i}$ , where  $i = 1, \dots, L$ . We follow both the temporal growth and the spatial spread of a perturbation originating from site  $j$  by means of the classical OTOCs defined as

$$D_{n,ij} := \left| \frac{\delta x_{n,i}}{\delta x_{0,j}} \right| \quad \text{and} \quad \tilde{D}_{n,ij} := \left\langle \left| \frac{\delta x_{n,i}}{\delta x_{0,j}} \right| \right\rangle_r, \quad (8)$$

in the deterministic case ( $r = 0$ ) and in the presence of resetting ( $r > 0$ ), respectively. To make analytical progress, we assume that the OTOC of the deterministic dynamics takes the form

$$D_{n,ij} \propto \exp \left[ \lambda \left( \frac{|i-j|}{n} \right) n \right] \quad (9)$$

for  $n \geq |i-j|$ , and  $D_{n,ij} = 0$  otherwise. Here, the function  $\lambda(v)$  is commonly referred to as a velocity-dependent Lyapunov exponent. This ansatz is known to capture the phenomenology in a wide class of models [23, 70–72]. We assume that  $\lambda(v)$  is a continuous monotonically decreasing function with negative curvature,  $\lambda(0) > 0$ , and that  $\lambda(v)$  crosses zero at a finite velocity  $v_B$ . At large times, this ansatz describes a traveling wavefront that propagates ballistically at the so-called butterfly velocity  $v_B = \lambda^{-1}(0)$ , where  $\lambda^{-1}$  denotes the inverse function of  $\lambda$ . At this front, the exponential growth of the OTOC is characterized by the Lyapunov rate  $\lambda_B = -v_B \lambda'(v_B) > 0$  [61]. Similarly to Eq. (4), the OTOC satisfies the following renewal equation for  $n \geq 1$

$$\tilde{D}_{n,ij} = \sum_{m=0}^{n-1} r(1-r)^m D_{m,ij} + (1-r)^n D_{n,ij}. \quad (10)$$

This allows the computation of OTOCs in the presence of stochastic resetting using exclusively data from the deterministic map, thereby avoiding the need for intricate averaging over resetting histories.

In the thermodynamics limit  $L \rightarrow \infty$  and at large times, we identify a traveling wavefront propagating at the renormalized butterfly velocity

$$\tilde{v}_B = \begin{cases} \lambda^{-1}(-\log(1-r)) & \text{if } r < r_c \\ 0 & \text{if } r \geq r_c, \end{cases} \quad (11)$$

where the critical resetting rate is given by  $r_c = 1 - e^{-\lambda(0)}$ . Without loss of generality, we momentarily simplify the notation by taking the initial perturbation at the site  $j = 1$  and dropping the  $j$  index. The geometry of the wavefront can be computed by re-expressing the renewal equation in the frame moving at velocity  $\tilde{v}_B$ , *i.e.* setting  $i = \tilde{v}_B n + 1 + k$  where  $k$  is spatial coordinate in the moving frame. When  $\tilde{v}_B n \gg |k|$ , we obtain the front shape

$$\lim_{n \rightarrow \infty} \tilde{D}_{n, \tilde{v}_B n + k} = \exp(-k \tilde{\lambda}_B / \tilde{v}_B). \quad (12)$$

where the growth rate of the OTOC at the front is characterized by the renormalized Lyapunov exponent

$$\tilde{\lambda}_B = -\tilde{v}_B \lambda'(\tilde{v}_B). \quad (13)$$

In the phase  $r < r_c$ , both the butterfly velocity and the Lyapunov are reduced by stochastic resetting. The near-critical behavior is governed by the behavior of  $\lambda(v)$  in the vicinity of  $v = 0$ . Assuming it is described by  $\lambda(v) - \lambda(0) \sim v^\alpha$  where  $\alpha \geq 1$ , the renormalized butterfly

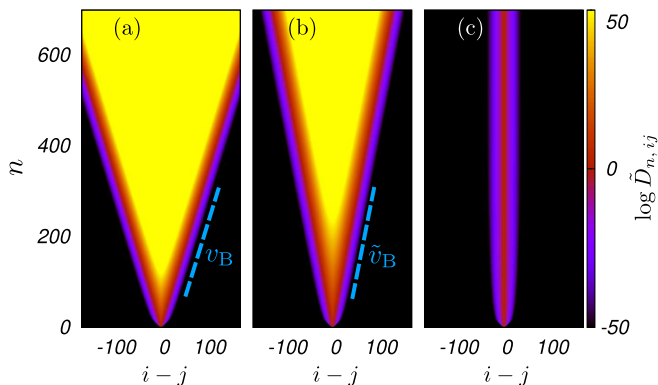


FIG. 2. Coupled logistic map [Eq. (14)] subject to stochastic resetting: the OTOC  $\tilde{D}_{n,ij}$  as a function of space and time reveals the ballistic spreading of perturbations. (a) Deterministic case,  $r = 0$ . (b) Finite resetting rate  $r = 0.2 < r_c \approx 0.38$ . (c)  $r = 0.4 > r_c$ . The butterfly velocities can be extracted from the slopes of the light cones. Lattice size  $L = 701$ ,  $\alpha = 4$ , and  $c = 0.1$ . The data is averaged over the initial perturbation site  $j$ , ranging from 1 to  $L$ .

velocity and Lyapunov exponent scale as  $\tilde{v}_B \sim (r_c - r)^\alpha$  and  $\tilde{\lambda}_B \sim (r_c - r)^{\alpha^2}$ . In the phase  $r > r_c$ , the resetting rate becomes sufficiently strong to drive a dynamical phase transition where the dynamics become non-chaotic, non-ergodic and the spread of information is brought to a complete arrest. Explicit computations and additional details are provided in the Supplementary Material [61].

We illustrate our findings using the coupled logistic map, a one-dimensional lattice of logistic maps interacting with their nearest neighbors. In the absence of resetting, the deterministic dynamics are generated by

$$x_{n+1,i} = f(x_{n,i}) + \frac{c}{2} [f(x_{n,i-1}) - 2f(x_{n,i}) + f(x_{n,i+1})], \quad (14)$$

with periodic boundary conditions. The first onsite term is precisely the nonlinearity in Eq. (7). The second term can be seen as a discrete Laplace operator with the diffusive coupling  $c \in [0, 1]$ . We use a single initial state with random  $x_{0,i} \in [0, 1]$  for  $i = 1, \dots, L$ . The map preserves  $x_{n,i} \in [0, 1]$  at all times. The coupled logistic map exhibits a rich phase diagram and has been widely studied in the context of spatiotemporal chaos, addressing phenomena such as spatial bifurcation, pattern selection, spatiotemporal intermittency, and soliton turbulence [67–69, 73–75]. Here, we fix  $\alpha = 4$  and  $c = 0.1$ , corresponding to a regime of fully developed turbulence. Additional details are provided in the supplementary material [61]. In the presence of resetting, the OTOCs are numerically obtained with the renewal formula in Eq. (10), making use of the OTOCs of the deterministic map. The latter are computed using an algorithm discussed in the Supplementary Material [61]. To avoid boundary effects, we restrict times to  $2n < L$ .

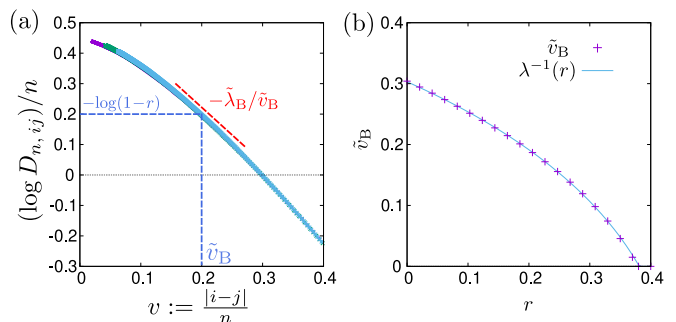


FIG. 3. Spatiotemporal chaos in the logistic map lattice subject to stochastic resetting. (a) The velocity-dependent Lyapunov  $\lambda(v)$  [Eq. (9)] is numerically extracted from the collapse of  $(\log D_{n,ij})/n$  versus  $v := |i-j|/n$  for various values of  $i-j$  in the deterministic case ( $r = 0$ ). The butterfly velocity  $\tilde{v}_B$  at  $r > 0$  can be determined by solving  $\lambda(\tilde{v}_B) = -\log(1-r)$ . The slope of  $\lambda(v)$  at this solution determines the Lyapunov rate  $\tilde{\lambda}_B$ . (b)  $\tilde{v}_B$  is extracted from the slope of the light cones (see Fig. 2) and is compared to the prediction of Eq. (11) as a function of the resetting rate  $r$ . Lattice size  $L = 701$ ,  $\alpha = 4$ , and  $c = 0.1$ .

Figure 2 illustrates the spatiotemporal behavior of the OTOC  $\tilde{D}_{n,ij}$  under different resetting conditions. Panel (a) shows the light-cone structure of the OTOC in the absence of resetting ( $r = 0$ ). The local perturbation of the initial condition evolves into a traveling wavefront that propagates ballistically at the butterfly velocity  $v_B$  visible as the slope of the light cone at late times. Note that the causal light cone at the maximal Lieb-Robinson velocity  $v_{LR} = 1$  can be seen at early times, and it is overshadowed by the prominence of the butterfly front at later times. In Panel (b), the butterfly velocity is visibly reduced by a finite resetting rate ( $r = 0.2$ ). In Panel (c), for  $r > r_c$ , the light cone collapses as the dynamics freeze, signaling the arrest of spatiotemporal chaos. Noteworthy, a similar dynamical phase transition was reported in deterministic classical many-body systems with kinetic constraints [12, 13].

In Fig. 3, we test the theoretical predictions of Eq. (11) for the reduction of the butterfly velocity by stochastic resetting. In panel (a), the velocity-dependent Lyapunov exponent  $\lambda(v)$  is extracted by collapsing the OTOC data at  $r = 0$  onto a single master curve, validating the ansatz in Eq. (9). In panel (b), we extract the butterfly velocities in the presence of resetting from the analysis of the light cones and compare them with the theoretical predictions of Eq. (11). The agreement between the numerical results and the analytical predictions is excellent.

*Discussions and outlook.*— We have shown that stochastic resetting provides a powerful mechanism for mitigating spatiotemporal chaos and can even induce a dynamical phase transition to a non-chaotic regime, where the spreading of information is brought to a complete halt. This can be put in perspective with the quantum many-body localized regimes where, although slower than ballistic, the spreading of information is thought to survive

in the absence of transport. More generally, the insights gained from these classical results will pave the path to understanding ergodicity and chaos in many-body quantum systems subject to resetting [76–79]. While we focused on discrete nonlinear maps, our results readily adapt to continuous-time dynamics. Using the dictionary  $\lambda \rightarrow \lambda dt$  and  $r \rightarrow r dt$ , the renormalized Lyapunov in Eq. (5) becomes  $\tilde{\lambda} = \lambda - r$ , the butterfly velocity in Eq. (11) becomes  $\tilde{v}_B = \lambda^{-1}(r)$ , and the expression of  $\tilde{\lambda}_B$  in (13) remains valid, see Ref. [61] for more details. The versatility of these results suggests the possibility of developing a geometrical optics theory to investigate phenomena such as the refraction of “information light rays” on spatial domains subject to resetting.

Acknowledgements.– M.K. acknowledges support from the Department of Atomic Energy, Government of In-

dia, under project No. RTI4001. M.K. also thanks the VAJRA faculty scheme (No. VJR/2019/000079) from the Science and Engineering Research Board (SERB), Department of Science and Technology, Government of India. We gratefully acknowledge support from the International Research Project (IRP) titled ‘Classical and Quantum Dynamics in Out of Equilibrium Systems’ (Dy-noutSys), funded by CNRS, France. M.K. thanks the Institute of Physics at EPFL in Lausanne for their hospitality. C.A. thanks the International Centre for Theoretical Sciences (ICTS) in Bangalore for their hospitality. This research was supported in part by the ICTS and CE-FIPRA for participating in the “Indo-French Workshop on Classical and quantum dynamics in out of equilibrium systems” (ICTS/IFWCQM2024/12).

- 
- [1] S. H. Shenker and D. Stanford, Black holes and the butterfly effect, *Journal of High Energy Physics* **2014**, 67 (2014).
- [2] J. Maldacena, S. H. Shenker, and D. Stanford, A bound on chaos, *Journal of High Energy Physics* **2016**, 106 (2016).
- [3] D. A. Roberts and B. Swingle, Lieb-robinson bound and the butterfly effect in quantum field theories, *Physical Review Letters* **117**, 091602 (2016).
- [4] A. Bohrdt, C. B. Mendl, M. Endres, and M. Knap, Scrambling and thermalization in a diffusive quantum many-body system, *New Journal of Physics* **19**, 063001 (2017).
- [5] B. Swingle, G. Bentsen, M. Schleier-Smith, and P. Hayden, Measuring the scrambling of quantum information, *Physical Review A* **94**, 040302 (2016).
- [6] J. Cohen, A. Petrescu, R. Shillito, and A. Blais, Reminiscence of classical chaos in driven transmons, *PRX Quantum* **4**, 020312 (2023).
- [7] E. M. Bollt, Review of chaos communication by feedback control of symbolic dynamics, *International Journal of Bifurcation and Chaos* **13**, 269 (2003).
- [8] S. Boccaletti, C. Grebogi, Y.-C. Lai, H. Mancini, and D. Maza, The control of chaos: theory and applications, *Physics Reports* **329**, 103 (2000).
- [9] I. Antoniou, V. Basios, and F. Bosco, Probabilistic control of chaos: Chaotic maps under control, *Computers & Mathematics with Applications* **34**, 373 (1997).
- [10] T. Iadecola, S. Ganeshan, J. H. Pixley, and J. H. Wilson, Dynamical entanglement transition in the probabilistic control of chaos (2022), [arXiv:2207.12415 \[cond-mat.dis-nn\]](https://arxiv.org/abs/2207.12415).
- [11] H. Pan, S. Ganeshan, T. Iadecola, J. H. Wilson, and J. H. Pixley, Local and nonlocal stochastic control of quantum chaos: Measurement- and control-induced criticality, *Physical Review B* **110**, 054308 (2024).
- [12] A. Deger, S. Roy, and A. Lazarides, Arresting classical many-body chaos by kinetic constraints, *Physical Review Letters* **129**, 160601 (2022).
- [13] A. Deger, A. Lazarides, and S. Roy, Constrained dynamics and directed percolation, *Physical Review Letters* **129**, 190601 (2022).
- [14] A. I. Larkin and Y. N. Ovchinnikov, Quasiclassical Method in the Theory of Superconductivity, *Soviet Journal of Experimental and Theoretical Physics* **28**, 1200 (1969).
- [15] D. J. Luitz and Y. Bar Lev, Information propagation in isolated quantum systems, *Phys. Rev. B* **96**, 020406 (2017).
- [16] S. Nakamura, E. Iyoda, T. Deguchi, and T. Sagawa, Universal scrambling in gapless quantum spin chains, *Physical Review B* **99**, 224305 (2019).
- [17] A. Das, S. Chakrabarty, A. Dhar, A. Kundu, D. A. Huse, R. Moessner, S. S. Ray, and S. Bhattacharjee, Light-Cone Spreading of Perturbations and the Butterfly Effect in a Classical Spin Chain, *Physical Review Letters* **121**, 024101 (2018).
- [18] S. D. Murugan, D. Kumar, S. Bhattacharjee, and S. S. Ray, Many-body chaos in thermalized fluids, *Physical Review Letters* **127**, 124501 (2021).
- [19] T. Bilitewski, S. Bhattacharjee, and R. Moessner, Temperature Dependence of the Butterfly Effect in a Classical Many-Body System, *Physical Review Letters* **121**, 250602 (2018).
- [20] T. Bilitewski, S. Bhattacharjee, and R. Moessner, Classical many-body chaos with and without quasiparticles, *Physical Review B* **103**, 174302 (2021).
- [21] M. Kumar, A. Kundu, M. Kulkarni, D. A. Huse, and A. Dhar, Transport, correlations, and chaos in a classical disordered anharmonic chain, *Physical Review E* **102**, 022130 (2020).
- [22] A. K. Chatterjee, M. Kulkarni, and A. Kundu, Dynamical regimes of finite-temperature discrete nonlinear Schrödinger chain, *Physical Review E* **104**, 044136 (2021).
- [23] A. K. Chatterjee, A. Kundu, and M. Kulkarni, Spatiotemporal spread of perturbations in a driven dissipative duffing chain: An out-of-time-ordered correlator approach, *Physical Review E* **102**, 052103 (2020).
- [24] V. Khemani, D. A. Huse, and A. Nahum, Velocity-dependent Lyapunov exponents in many-body quantum, semiclassical, and classical chaos, *Physical Review B* **98**, 144304 (2018).
- [25] D. Roy, D. A. Huse, and M. Kulkarni, Out-of-time-

- ordered correlator in the one-dimensional kuramoto-sivashinsky and kardar-parisi-zhang equations, *Physical Review E* **108**, 054112 (2023).
- [26] B. S. Kiran, D. A. Huse, and M. Kulkarni, Spatiotemporal spread of perturbations in power-law models at low temperatures: Exact results for classical out-of-time-order correlators, *Physical Review E* **104**, 044117 (2021).
- [27] B. Swingle and D. Chowdhury, Slow scrambling in disordered quantum systems, *Physical Review B* **95**, 060201 (2017).
- [28] R.-Q. He and Z.-Y. Lu, Characterizing many-body localization by out-of-time-ordered correlation, *Physical Review B* **95**, 054201 (2017).
- [29] Y. Liao and V. Galitski, Nonlinear sigma model approach to many-body quantum chaos: Regularized and unregularized out-of-time-ordered correlators, *Physical Review B* **98**, 205124 (2018).
- [30] C. Aron, E. Brunet, and A. Mitra, Kinetics of information scrambling in correlated metals: Disorder-driven transition from shock wave to Fisher or Kolmogorov-Petrovsky-Piskunov dynamics, *Physical Review B* **108**, L241106 (2023).
- [31] C. Rangi, J. Moreno, and K.-M. Tam, Out of time order correlation of the hubbard model with random local disorder (2024), [arXiv:2403.03214 \[cond-mat.str-el\]](https://arxiv.org/abs/2403.03214).
- [32] M. R. Evans and S. N. Majumdar, Diffusion with stochastic resetting, *Physical Review Letters* **106**, 160601 (2011).
- [33] M. R. Evans and S. N. Majumdar, Diffusion with optimal resetting, *Journal of Physics A: Mathematical and Theoretical* **44**, 435001 (2011).
- [34] M. R. Evans and S. N. Majumdar, Diffusion with resetting in arbitrary spatial dimension, *Journal of Physics A: Mathematical and Theoretical* **47**, 285001 (2014).
- [35] M. R. Evans, S. N. Majumdar, and G. Schehr, Stochastic resetting and applications, *Journal of Physics A: Mathematical and Theoretical* **53**, 193001 (2020).
- [36] S. Gupta and A. M. Jayannavar, Stochastic resetting: A (very) brief review, *Frontiers in Physics* **10**, 10.3389/fphy.2022.789097 (2022).
- [37] F. Faisant, B. Besga, A. Petrosyan, S. Ciliberto, and S. N. Majumdar, Optimal mean first-passage time of a brownian searcher with resetting in one and two dimensions: experiments, theory and numerical tests, *Journal of Statistical Mechanics: Theory and Experiment* **2021**, 113203 (2021).
- [38] O. Tal-Friedman, A. Pal, A. Sekhon, S. Reuveni, and Y. Roichman, Experimental realization of diffusion with stochastic resetting, *The Journal of Physical Chemistry Letters* **11**, 7350 (2020).
- [39] B. Besga, A. Bovon, A. Petrosyan, S. N. Majumdar, and S. Ciliberto, Optimal mean first-passage time for a brownian searcher subjected to resetting: Experimental and theoretical results, *Physical Review Research* **2**, 032029 (2020).
- [40] M. R. Evans, S. N. Majumdar, and K. Mallick, Optimal diffusive search: nonequilibrium resetting versus equilibrium dynamics, *Journal of Physics A: Mathematical and Theoretical* **46**, 185001 (2013).
- [41] G. Mercado-Vásquez, D. Boyer, and S. N. Majumdar, Reducing mean first passage times with intermittent confining potentials: a realization of resetting processes, *Journal of Statistical Mechanics: Theory and Experiment* **2022**, 093202 (2022).
- [42] J. Fuchs, S. Goldt, and U. Seifert, Stochastic thermodynamics of resetting, *Europhysics Letters* **113**, 60009 (2016).
- [43] F. Mori, K. S. Olsen, and S. Krishnamurthy, Entropy production of resetting processes, *Physical Review Research* **5**, 023103 (2023).
- [44] A. Nagar and S. Gupta, Stochastic resetting in interacting particle systems: a review, *Journal of Physics A: Mathematical and Theoretical* **56**, 283001 (2023).
- [45] P. C. Bressloff, Kuramoto model with stochastic resetting and coupling through an external medium (2024), [arXiv:2411.15534 \[cond-mat.stat-mech\]](https://arxiv.org/abs/2411.15534).
- [46] M. Sarkar and S. Gupta, Synchronization in the kuramoto model in presence of stochastic resetting, *Chaos: An Interdisciplinary Journal of Nonlinear Science* **32**, 073109 (2022).
- [47] P. C. Bressloff, Kuramoto model with stochastic resetting and coupling through an external medium (2024), [arXiv:2411.15534 \[cond-mat.stat-mech\]](https://arxiv.org/abs/2411.15534).
- [48] P. C. Bressloff, Global density equations for interacting particle systems with stochastic resetting: from overdamped brownian motion to phase synchronization (2024), [arXiv:2401.03501 \[cond-mat.stat-mech\]](https://arxiv.org/abs/2401.03501).
- [49] S. Gupta, S. N. Majumdar, and G. Schehr, Fluctuating interfaces subject to stochastic resetting, *Physical Review Letters* **112**, 220601 (2014).
- [50] U. Basu, A. Kundu, and A. Pal, Symmetric exclusion process under stochastic resetting, *Physical Review E* **100**, 032136 (2019).
- [51] O. Sadekar and U. Basu, Zero-current nonequilibrium state in symmetric exclusion process with dichotomous stochastic resetting, *Journal of Statistical Mechanics: Theory and Experiment* **2020**, 073209 (2020).
- [52] S. Karthika and A. Nagar, Totally asymmetric simple exclusion process with resetting, *Journal of Physics A: Mathematical and Theoretical* **53**, 115003 (2020).
- [53] M. Magoni, S. N. Majumdar, and G. Schehr, Ising model with stochastic resetting, *Physical Review Research* **2**, 033182 (2020).
- [54] C. Aron and M. Kulkarni, Nonanalytic nonequilibrium field theory: Stochastic reheating of the Ising model, *Physical Review Research* **2**, 043390 (2020).
- [55] M. Biroli, H. Larralde, S. N. Majumdar, and G. Schehr, Extreme statistics and spacing distribution in a brownian gas correlated by resetting, *Physical Review Letters* **130**, 207101 (2023).
- [56] M. Biroli, H. Larralde, S. N. Majumdar, and G. Schehr, Exact extreme, order, and sum statistics in a class of strongly correlated systems, *Phys. Rev. E* **109**, 014101 (2024).
- [57] M. Kulkarni, S. N. Majumdar, and S. Sabhapandit, Dynamically emergent correlations in bosons via quantum resetting (2024), [arXiv:2407.20342 \[cond-mat.quant-gas\]](https://arxiv.org/abs/2407.20342).
- [58] S. H. Strogatz, *Nonlinear dynamics and chaos: with applications to physics, biology, chemistry, and engineering* (CRC press, 2018).
- [59] J. M. T. Thompson and H. B. Stewart, *Nonlinear dynamics and chaos* (John Wiley & Sons, 2002).
- [60] R. C. Hilborn, *Chaos and nonlinear dynamics: an introduction for scientists and engineers* (Oxford university press, 2000).
- [61] See Supplementary Material.
- [62] E. N. Lorenz, The problem of deducing the climate from the governing equations, *Tellus* **16**, 1 (1964).

- [63] R. M. May, Simple mathematical models with very complicated dynamics, *Nature (London)* **261**, 459 (1976).
- [64] J. L. McCauley, *Chaos, dynamics, and fractals: an algorithmic approach to deterministic chaos*, Vol. 2 (Cambridge University Press, 1993).
- [65] M. Ausloos and M. Dirickx, *The logistic map and the route to chaos: From the beginnings to modern applications* (Springer Science & Business Media, 2006).
- [66] S. Ulam and J. Von Neumann, On combination of stochastic and deterministic processes, *bulletin amer. Math. Soc* **53**, 1120 (1947).
- [67] K. Kaneko, Overview of coupled map lattices, *Chaos: An Interdisciplinary Journal of Nonlinear Science* **2**, 279 (1992).
- [68] K. Kaneko, Spatiotemporal chaos in one- and two-dimensional coupled map lattices, *Physica D: Nonlinear Phenomena* **37**, 60 (1989).
- [69] J.-R. Chazottes and B. Fernandez, *Dynamics of coupled map lattices and of related spatially extended systems*, Vol. 671 (Springer Science & Business Media, 2005).
- [70] K. Kaneko, Lyapunov analysis and information flow in coupled map lattices, *Physica D: Nonlinear Phenomena* **23**, 436 (1986).
- [71] R. J. Deissler and K. Kaneko, Velocity-dependent lyapunov exponents as a measure of chaos for open-flow systems, *Physics Letters A* **119**, 397 (1987).
- [72] V. Khemani, D. A. Huse, and A. Nahum, Velocity-dependent lyapunov exponents in many-body quantum, semiclassical, and classical chaos, *Physical Review B* **98**, 144304 (2018).
- [73] A. M. Hagerstrom, T. E. Murphy, R. Roy, P. Hövel, I. Omelchenko, and E. Schöll, Experimental observation of chimeras in coupled-map lattices, *Nature Physics* **8**, 658 (2012).
- [74] J. Losson and M. C. Mackey, Thermodynamic properties of coupled map lattices, *Stochastic and Spatial Structures of Dynamical Systems*, North-Holland, Amsterdam (1996).
- [75] P. Muruganandam and M. Senthilvelan, Manifestation of strange nonchaotic attractors in extended systems: a study through out-of-time-ordered correlators, *The European Physical Journal B* **95**, 124 (2022).
- [76] B. Mukherjee, K. Sengupta, and S. N. Majumdar, Quantum dynamics with stochastic reset, *Physical Review B* **98**, 104309 (2018).
- [77] D. C. Rose, H. Touchette, I. Lesanovsky, and J. P. Garrahan, Spectral properties of simple classical and quantum reset processes, *Physical Review E* **98**, 022129 (2018).
- [78] M. Magoni, F. Carollo, G. Peretto, and I. Lesanovsky, Emergent quantum correlations and collective behavior in noninteracting quantum systems subject to stochastic resetting, *Physical Review A* **106**, 052210 (2022).
- [79] M. Kulkarni and S. N. Majumdar, Generating entanglement by quantum resetting, *Physical Review A* **108**, 062210 (2023).

## Supplementary Material

### I. DISCRETE-TIME MAPS SUBJECT TO STOCHASTIC RESETTING

#### A. Stationary distribution of the deterministic map

Let us first briefly discuss the deterministic case, in the absence of resetting ( $r = 0$ ). We consider a zero-dimensional map of the form

$$x_n \mapsto x_{n+1} = f(x_n), \quad (\text{S1})$$

where  $f(x)$  is a nonlinear function of  $x$  and  $n \geq 0$ . We assume that the deterministic map has a unique stationary distribution  $p_{\text{st}}(x)$  and that the dynamics are ergodic. The ergodic theorem ensures that

$$p_{\text{st}}(x) = \lim_{N \rightarrow \infty} \frac{1}{N+1} \sum_{n=0}^N \delta(x - x_n) \quad (\text{S2})$$

and  $p_{\text{st}}(x) > 0$  for all  $x$ , *i.e.*, any region of phase space will be visited with finite frequency. Note that the expression above is “democratic” in the sense that it is invariant under any permutation of the  $x_n$ ’s.

#### B. Stationary distribution with stochastic resetting

In the presence of a finite resetting rate ( $0 < r < 1$ ), the dynamics are generated by the following stochastic map

$$x_n \mapsto x_{n+1} = \begin{cases} f(x_n) & \text{with probability } 1 - r \\ x_0 & \text{with probability } r. \end{cases} \quad (\text{S3})$$

The corresponding stationary distribution, if it exists, is given by the time-averaged distribution  $\frac{1}{m+1} \sum_{n=0}^m \delta(x - x_n)$  truncated at the time  $m$  where resetting occurs, and averaged over all possible resetting times:

$$\tilde{p}_{\text{st}}(x) = \sum_{m=0}^{\infty} P_m \frac{1}{m+1} \sum_{n=0}^m \delta(x - x_n) \quad (\text{S4})$$

with  $P_m := r(1-r)^m$  the probability of a reset immediately after  $m$  time steps without reset. Standard algebra yields

$$\tilde{p}_{\text{st}}(x) = \sum_{n=0}^{\infty} \tilde{g}_n \delta(x - x_n), \quad (\text{S5})$$

with  $\tilde{g}_n := r(1-r)^n \Phi(1-r, 1, 1+n)$  where  $\Phi$  is the Hurwitz–Lerch transcendent.  $g_n$  is monotonously decreasing with  $n$  and  $\tilde{g}_n \sim \exp(-rn)/n$  at large  $n$ . One may check the normalization

$$\int dx \tilde{p}_{\text{st}}(x) = \sum_{n=0}^{\infty} \tilde{g}_n = 1. \quad (\text{S6})$$

Resetting is naturally expected to enhance the overall time spent by the system in the initial state,  $x_0$ , and its first subsequent images under the map  $f$ . This is confirmed by examining Eq. (S5), which, unlike the deterministic case in Eq. (S2), lacks invariance under arbitrary permutations of the  $x_n$ ’s. Notably, the initial condition exhibits the highest weight to the stationary distribution  $\tilde{p}_{\text{st}}(x)$ , given by  $\tilde{g}_0 = \frac{r}{1-r} \log(1/r)$ . This demonstrates the dependence of the stationary distribution  $\tilde{p}_{\text{st}}(x)$  on the choice of the initial condition.

If, additionally, one averages the resetting dynamics over the initial conditions by sampling  $x_0$  from the stationary distribution of the deterministic map, *i.e.*, with probability  $p_{\text{st}}(x_0)$ , one can show by induction that  $p_{\text{st}}(x)$  remains an invariant distribution of the resetting dynamics. Assume that  $x_n$  is sampled from  $p_{\text{st}}$ .

- If there is no resetting at time  $n+1$ , then  $x_{n+1} = f(x_n)$  is also sampled from  $p_{\text{st}}$  since  $p_{\text{st}}$  is precisely the invariant distribution of the deterministic map.



- If there is a resetting event at time  $n + 1$ , then  $x_{n+1} = x_0$ , which is also sampled from  $p_{\text{st}}$  by construction.

In both cases,  $x_{n+1}$  is sampled from  $p_{\text{st}}$ . Since this holds true for  $n = 0$  (by the initial sampling of  $x_0$ ), it holds true for all times  $n \geq 0$  by induction.

This remarkable result states that, under such an averaging procedure of the initial conditions, the statics of the map are not altered by stochastic resetting. For instance, this implies that the celebrated bifurcation diagram of the logistic map is not altered by stochastic resetting. However, in this work, we do not perform this additional averaging over the initial conditions. Instead, we focus on the case of a single, arbitrary, initial condition  $x_0$ . We have carefully checked that our results do not depend on the choice of  $x_0$ .

### C. Ergodicity with stochastic resetting

Here, we provide semi-rigorous arguments to assess the ergodicity of the dynamics subject to stochastic resetting, assuming that the deterministic dynamics are ergodic in a bounded phase space and chaotic with a finite Lyapunov exponent  $\lambda > 0$ . We caution that the results presented below should only be regarded as indicative until this problem receives a fully rigorous analysis.

Ergodicity of the deterministic map, *i.e.*  $p_{\text{st}}(x) > 0$  for arbitrary generic values of  $x$ , implies that for a given small  $\epsilon > 0$ , and a large enough time  $N$ , the condition  $|x - x_n| < \epsilon$  is met by a finite set  $\Lambda_{\epsilon, N}(x)$  of  $n$ 's along the trajectory before time  $N$  is reached. The size of this set is on the order of  $\mathcal{O}(\epsilon \times N)$ . In practice, we question whether the stationary distribution in the presence of stochastic resetting  $\tilde{p}_{\text{st}}(x) > 0$  for arbitrary generic values of  $x$ . Integrating Eq. (S5) on a small interval of length  $2\epsilon$  around  $x$ , we get

$$\int_{x-\epsilon}^{x+\epsilon} dy \tilde{p}_{\text{st}}(y) = \sum_{n \in \Lambda_{\epsilon}(y)} \tilde{g}_n, \quad (\text{S7})$$

where the infinite set that appears in the summation  $\Lambda_{\epsilon}(x) := \lim_{N \rightarrow \infty} \Lambda_{\epsilon, N}(x)$  collects all the times at which a given trajectory, initialized at  $x_0$ , comes at a distance  $\epsilon$  of the target  $x$ . For  $\epsilon$  small enough, this yields

$$\tilde{p}_{\text{st}}(x) = \frac{1}{2\epsilon} \sum_{n \in \Lambda_{\epsilon}(x)} \tilde{g}_n. \quad (\text{S8})$$

All the  $g_n$ 's being strictly positive, we may therefore find a lower bound to the sum over the infinite set  $\Lambda_{\epsilon}(x)$  by keeping a single term only:

$$\tilde{p}_{\text{st}}(x) > \frac{1}{2\epsilon} \tilde{g}_{n_{\text{min}}}, \quad (\text{S9})$$

where  $n_{\text{min}}$  is chosen to be the smallest element of  $\Lambda_{\epsilon}(x)$ , corresponding to the largest weight  $\tilde{g}_n$  of the sum in Eq. (S8). We now use the chaotic character of the deterministic dynamics to get an estimate for  $n_{\text{min}}$ : the typical distance between two trajectories originating from neighboring initial conditions at a small enough distance  $\epsilon$  grows exponentially

$$\frac{|\delta x_n|}{\epsilon} \sim e^{\lambda n} \text{ at large enough } n, \quad (\text{S10})$$

with the Lyapunov exponent  $\lambda > 0$ . Identifying  $|\delta x_n|$  with the typical size of phase space (assumed to be bounded), the waiting time of a time-reversed trajectory to come at a close distance  $\epsilon$  of the target  $x$  can be estimated as

$$n_{\text{min}} \sim \frac{1}{\lambda} \log \frac{1}{\epsilon}. \quad (\text{S11})$$

Using the asymptotic expression of  $\tilde{g}_n$ , this yields the bound

$$\tilde{p}_{\text{st}}(x) \gtrsim \frac{\lambda}{2 \log 1/\epsilon} \left( \frac{1}{\epsilon} \right)^{\frac{\log(1-r)}{\lambda} + 1}. \quad (\text{S12})$$

Inspection of the right-hand side of the above inequality indicates a drastic change in the ergodic nature when the exponent  $\frac{\log(1-r)}{\lambda} + 1$  vanishes. This occurs precisely at the critical resetting rate  $r_c = e^{-\lambda} - 1$ , where the renormalized Lyapunov exponent  $\tilde{\lambda}$  vanishes. The remarkable concurrence of these two transitions leads us to propose the following conjecture: For  $r < r_c$ , the dynamics are ergodic, whereas ergodicity is lost for  $r > r_c$ .

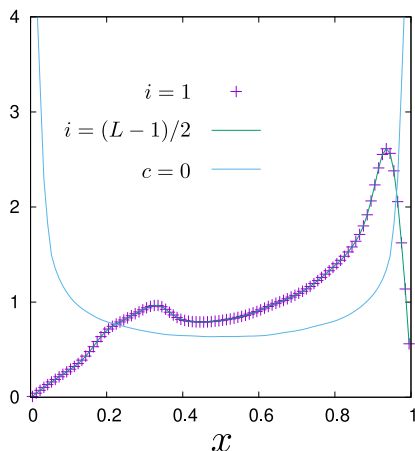


FIG. S1. Coupled logistic map with  $\alpha = 4$  and  $c = 0.1$  (no resetting,  $r = 0$ ): the local marginal of the stationary distribution is identical at all sites, here  $i = 1$  and  $i = (L - 1)/2$ . The stationary distribution of the corresponding logistic map ( $c = 0$ ),  $p_{\text{st}}(x) = 1/(\pi\sqrt{x(1-x)})$ , is plotted for comparison. Lattice size  $L = 701$ .

## II. DETERMINISTIC COUPLED LOGISTIC MAP

In this Section, we briefly present the coupled logistic map in the absence of stochastic resetting ( $r = 0$ ) and explain how to efficiently compute the corresponding OTOC  $D_{n,ij}$  introduced in Eq. (8) of the main manuscript, circumventing the delicate numerical computation of linear responses to infinitesimal perturbations. The OTOC in the presence of resetting,  $\tilde{D}_{n,ij}$ , is obtained by means of the renewal formula in Eq. (10) which circumvents the delicate average over resetting trajectories.

The coupled logistic map consists of a one-dimensional chain of  $L$  sites where each site hosts a single logistic map that interacts diffusively with its nearest neighbors. At time  $n = 0$ , the state of the system is specified by the vector  $x_0 = \{x_{0,i}\}_{i=1\dots L}$  with  $|x_{0,i}| \leq 1$ . The deterministic dynamics are generated by

$$x_{n+1,i} = F_i(x_n), \quad (\text{S13})$$

with the nonlinear vector map

$$F_i(x_n) = f(x_{n,i}) + \frac{c}{2} [f(x_{n,i-1}) - 2f(x_{n,i}) + f(x_{n,i+1})], \quad (\text{S14})$$

together with periodic boundary conditions. Here,  $f(x) = \alpha x(1-x)$  is the logistic function with the parameter  $\alpha \in [0, 4]$  and  $0 < c < 1$  is a diffusion parameter. This ensures the multidimensional interval  $[0, 1]^L$  is stable under the coupled logistic map. In practice, we work with  $\alpha = 4$  and  $c = 0.1$  for which we have carefully checked that the deterministic dynamics reach a stationary state that is both uniform in space and time. This is illustrated in Fig. S1 where the local marginal of the stationary distribution is plotted at sites  $i = 1$  and  $i = (L - 1)/2$ . For comparison, we also plot  $p_{\text{st}}(x) = 1/(\pi\sqrt{x(1-x)})$  which is the stationary distribution of the logistic map (at  $c = 0$ ).

The OTOC of the deterministic dynamics is defined as

$$D_{n,ij} = \left| \frac{\delta x_{n,i}}{\delta x_{0,j}} \right|. \quad (\text{S15})$$

At  $n = 0$ , this is simply  $D_{0,ij} = \delta_{ij}$ . For  $n \geq 1$ , the chain rule offers a convenient representation as a matrix product

$$D_{n,ij} = |\{F'(x_0) \times F'(x_1) \times \dots \times F'(x_{n-1})\}_{ij}|, \quad (\text{S16})$$

where we introduced the Jacobian matrix

$$F'_{ij}(x_n) := \frac{\partial F_i(x_n)}{\partial x_{n,j}}, \quad (\text{S17})$$

and  $\times$  denotes matrix multiplication in the spatial indices. In the particular case of the logistic lattice, we have

$$F'_{ij}(x) = (1-c) \frac{\partial f(x_i)}{\partial x_j} \delta_{ij} + \frac{c}{2} \left[ \frac{\partial f(x_i)}{\partial x_{j+1}} \delta_{i,j+1} + \frac{\partial f(x_i)}{\partial x_{j-1}} \delta_{i,j-1} \right], \quad (\text{S18})$$

together with periodic boundary conditions.

### III. CONTINUOUS-TIME DYNAMICS SUBJECT TO STOCHASTIC RESETTING

In this Section, we formulate the resetting dynamics for dynamical systems with a continuous-time description. Although very similar to the discrete-time case, we find the continuous-time case more amenable for presenting analytical proofs.

#### A. Zero-dimensional systems (no space)

To simplify the discussion, we use similar notations and the following dictionary between the discrete-time and the continuous-time formulations:

$$\begin{aligned} n &\longleftrightarrow t/dt & \lambda &\longleftrightarrow \lambda dt \\ x_n &\longleftrightarrow x(t) & r &\longleftrightarrow r dt \\ x_{n+1} - x_n &\longleftrightarrow \partial_t x(t) & (1-r)^n &\longleftrightarrow e^{-rt} \end{aligned} \quad (\text{S19})$$

where  $\lambda$  and  $r$  are now rates instead of dimensionless exponent and probability, respectively. In particular, the resetting rate  $r$  now takes values in  $[0, \infty)$ .

##### 1. Deterministic dynamics & Lyapunov rate

Let us consider deterministic dynamics governed by the following first-order PDE

$$\partial_t x(t) = f(x(t)), \quad (\text{S20})$$

where  $f(x)$  is a non-linear function of  $x$  which is assumed to generate ergodic and chaotic dynamics.

The absolute distance between two trajectories starting from neighboring initial conditions is defined as

$$d(t) := \left| \frac{\delta x(t)}{\delta x(0)} \right|. \quad (\text{S21})$$

To make the connection with the study of quantum chaos, the quantity  $d(t)$  can be referred to as an ‘‘out-of-time-order correlator’’ (OTOC). Indeed, in a semi-classical sense,  $\delta x(t)/\delta x(0)$  is to be replaced by the commutator  $[\hat{x}(t), \hat{p}(0)]/i\hbar$  where  $\hat{p}$  is the momentum operator conjugated with the position operator  $\hat{x}$ ,  $[\hat{x}, \hat{p}] = i\hbar$ . Hence,  $d^2(t)$  is to be replaced by the square commutator  $\langle [\hat{x}(t), \hat{p}(0)]^\dagger [\hat{x}(t), \hat{p}(0)] \rangle / (i\hbar)^2$  where quantum mechanical operators explicitly appear out of time order and  $\langle \dots \rangle$  denotes averaging over an appropriately chosen initial density matrix.

The linearization of the deterministic dynamics for two close-by trajectories distant of  $\delta x(t)$  yields the first-order PDE

$$\partial_t \delta x(t) = \delta x(t) f'(x(t)), \quad (\text{S22})$$

which is solved as

$$d(t) = e^{\int_0^t d\tau |f'(x(\tau))|}. \quad (\text{S23})$$

The ergodic theorem notably ensures

$$\lim_{t \rightarrow \infty} \frac{1}{t} \int_0^t d\tau |f'(x(\tau))| = \int dx p_{\text{st}}(x) |f'(x)| =: \lambda > 0. \quad (\text{S24})$$

which provides a static definition of the Lyapunov rate. It connects to the traditional dynamical definition of the Lyapunov via the asymptotic expression at large times  $t \gg 1/\lambda$

$$d(t) \simeq e^{\lambda t}. \quad (\text{S25})$$

## 2. Dynamics subject to stochastic resetting & Lyapunov rate

In the presence of stochastic resetting, the dynamics are generated by

$$x(t + dt) = x(t) + f(x(t)) dt \quad \text{with probability } 1 - r dt \quad (\text{S26})$$

$$x(t + dt) = x(0) \quad \text{with probability } r dt. \quad (\text{S27})$$

We consider the OTOC

$$\tilde{d}(t) := \left\langle \left| \frac{\delta x(t)}{\delta x(0)} \right| \right\rangle_r, \quad (\text{S28})$$

where  $\langle \dots \rangle_r$  denotes the average with respect to the resetting events.  $\tilde{d}(t)$  can be simply related to its deterministic counterpart  $d(t)$  in Eq. (S21) via the following renewal formula

$$\tilde{d}(t) = r \int_0^t d\tau e^{-r\tau} d(\tau) + e^{-rt} d(t), \quad (\text{S29})$$

which is the continuous-time version of Eq. (4) in the main part of the manuscript. Using the solution in Eq. (S23), the renewal formula yields

$$\tilde{d}(t) = r \int_0^t d\tau e^{-r\tau + \int_0^\tau du |f'(x(u))|} + e^{-rt + \int_0^t d\tau |f'(x(\tau))|}. \quad (\text{S30})$$

Let us now divide the first time integral in Eq. (S30) as

$$\int_0^t d\tau = \int_0^{z(t)} d\tau + \int_{z(t)}^t d\tau, \quad (\text{S31})$$

where we introduced the *ad-hoc* timescale  $z(t) \gg 1/\lambda$  that is chosen to be monotonously growing slower than any power-law growth, *i.e.*  $\lim_{t \rightarrow \infty} z(t)/t^\alpha = 0 \forall \alpha > 0$ . Working at large time  $t$ , using the ergodic theorem in Eq. (S24) in the large time window  $[z(t), t]$ , we obtain the asymptotic expression

$$\tilde{d}(t) \simeq r \int_0^{z(t)} d\tau e^{-r\tau + \int_0^\tau du |f'(x(u))|} + \frac{r}{\lambda - r} \left[ e^{(\lambda - r)t} - e^{(\lambda - r)z(t)} \right] + e^{(\lambda - r)t}. \quad (\text{S32})$$

This asymptotic expression allows us to distinguish two dynamical regimes depending on the relative strength of the resetting rate  $r$  with the critical rate  $r_c = \lambda$ . If  $r < r_c$ , those of the terms above that involve  $z(t)$  are subdominant, and we obtain the exponential growth

$$\tilde{d}(t) \simeq \left( 1 + \frac{r}{\lambda} \right) e^{\tilde{\lambda} t}, \quad (\text{S33})$$

where the renormalized Lyapunov rate is given by

$$\tilde{\lambda} = \lambda - r > 0 \quad \text{if } r < r_c. \quad (\text{S34})$$

Noteworthy, the above asymptotic expression of  $\tilde{d}(t)$  and  $\tilde{\lambda}$  do not involve the details of the initial conditions. If  $r \geq r_c$ , the growth of  $\tilde{d}(t)$  in Eq. (S32) is sub-exponential and it can be described by a vanishing Lyapunov rate

$$\tilde{\lambda} = 0 \quad \text{if } r \geq r_c, \quad (\text{S35})$$

which is the signature of non-chaotic dynamics.

### B. Spatially extended systems

Here, we provide details on the continuous-time continuous-space formulation of the spatiotemporal spread of perturbation in extended systems subject to stochastic resetting. The state of the system is characterized by a spatially varying classical field which we denote by  $\phi(t, x)$  to avoid confusion (until now  $x$  denoted the state of the system, not the spatial position). The dictionary with the discrete-time formulation on the lattice is similar to the one in Sect. III A where, now,

$$\begin{aligned} x_{n,i} &\longleftrightarrow \phi(t, x) \\ \frac{x_{n,i-1} - 2x_{n,i} + x_{n,i+1}}{2} &\longleftrightarrow \nabla_x^2 \phi(t, x) \end{aligned} \quad (\text{S36})$$

### 1. Renewal formula for OTOCs

One defines the classical OTOCs for the deterministic dynamics and the resetting dynamics as, respectively,

$$D(t, x) := \left| \frac{\delta\phi(t, x)}{\delta\phi(0, 0)} \right| \quad \text{and} \quad \tilde{D}(t, x) := \left\langle \left| \frac{\delta\phi(t, x)}{\delta\phi(0, 0)} \right| \right\rangle_r. \quad (\text{S37})$$

Notably, these OTOCs obey a renewal equation that reads

$$\tilde{D}(t, x) = r \int_0^t d\tau e^{-r\tau} D(\tau, x) + e^{-rt} D(t, x). \quad (\text{S38})$$

### 2. “Light-ray” parametrization of the OTOC

Here, we assume that the spatiotemporal dependence of the OTOC of the deterministic dynamics is captured by the following ansatz,

$$D(t, x) = \exp\left(\lambda\left(\frac{x}{t}\right)t\right), \quad (\text{S39})$$

where the function  $\lambda(v)$  is commonly referred to as a velocity-dependent Lyapunov exponent. It is assumed to be a continuous monotonically decreasing function with negative curvature, with  $\lambda(0) > 0$  and  $\lambda(v)$  crosses zero at a finite velocity  $v_B$ :  $\lambda(v_B) = 0$ . In particular, on the light-ray traveling at the velocity  $v_B$ , this yields

$$D(t, x = v_B t) = 1. \quad (\text{S40})$$

Note that, although this is not explicit, the functional form in Eq. (S39) supports a traveling wavefront at the butterfly velocity  $v_B$ : take  $x = v_B t + z$  with  $|z| \ll v_B t$ , expand  $\lambda(v_B + z/t)$  to first order in  $z/t$ , and obtain the following traveling wavefront

$$D(t, x = v_B t + z) \xrightarrow{t \rightarrow \infty} \exp\left[-\frac{z}{v_B} \lambda_B\right], \quad (\text{S41})$$

where the Lyapunov rate  $\lambda_B := -v_B \lambda'(v_B) > 0$  sets the spatial extent of the exponentially-growing front.

### 3. Light-cone propagation with stochastic resetting

Here, we provide the derivations of the renormalized butterfly velocity that describes the effective speed of the ballistic spreading,

$$\tilde{v}_B = \begin{cases} \lambda^{-1}(r) & \text{if } r < r_c \\ 0 & \text{if } r \geq r_c, \end{cases} \quad (\text{S42})$$

where  $\lambda^{-1}$  is the functional inverse of the velocity-dependent Lyapunov introduced in Eq. (S39), as well as the renormalized Lyapunov that describes the spatial extent of the butterfly front,

$$\tilde{\lambda}_B = -\tilde{v}_B \lambda'(\tilde{v}_B). \quad (\text{S43})$$

Quite intuitively, we find both the butterfly velocity and the Lyapunov rate to be reduced by stochastic resetting:

$$\partial_r \tilde{v}_B \leq 0 \quad \text{and} \quad \partial_r \tilde{\lambda}_B \leq 0. \quad (\text{S44})$$

For simplicity of the algebra, we work in the framework of continuous-time dynamics, but the corresponding discrete-time expressions can be readily obtained without conceptual overhead. In practice, let us check that there is indeed a wavefront traveling at the velocity  $\tilde{v}_B = \lambda^{-1}(r)$  which, from now on, we assume to be finite. We explore the vicinity of the light ray at  $\tilde{v}_B$  by working with the parametrization  $x = \tilde{v}_B t + z$  and considering asymptotic times when  $|z| \ll v_B t$ . Using the renewal equation (S38) and the shorthand notation  $\tilde{\lambda}(v) := \lambda(v) - r$ , we have

$$\tilde{D}(t, x = \tilde{v}_B t + z) = r \int_0^t d\tau \exp\left[\tilde{\lambda}\left(\frac{\tilde{v}_B t + z}{\tau}\right)\tau\right] + \exp\left[\tilde{\lambda}\left(\frac{\tilde{v}_B t + z}{t}\right)t\right] \quad (\text{S45})$$

$$\simeq \exp\left[z\tilde{\lambda}'(\tilde{v}_B)\right] \left(1 + r \exp\left[-z\tilde{\lambda}'(\tilde{v}_B)\right] \int_0^t d\tau \exp\left[\tilde{\lambda}\left(\tilde{v}_B \frac{t}{\tau}\right)\tau + z\tilde{\lambda}'\left(\tilde{v}_B \frac{t}{\tau}\right)\right]\right), \quad (\text{S46})$$

where, in the second line, we expanded to first order in  $z$  and used  $\lambda(v_B) = 0$ . Performing the change of variable  $\tau \mapsto v := \tilde{v}_B t / \tau$  in the integral, we get

$$\tilde{D}(t, x = \tilde{v}_B t + z) \simeq \exp \left[ z \tilde{\lambda}'(\tilde{v}_B) \right] \left( 1 + r t \tilde{v}_B \exp \left[ -z \tilde{\lambda}'(\tilde{v}_B) \right] \int_{\tilde{v}_B}^{\infty} \frac{dv}{v^2} \exp \left[ \tilde{v}_B \frac{\tilde{\lambda}(v)}{v} t + z \tilde{\lambda}'(v) \right] \right). \quad (\text{S47})$$

Let us now take the limit  $t \rightarrow \infty$ . Note that the term  $\tilde{\lambda}(v)$  in the integrand above is always negative, since  $\tilde{\lambda}(v) := \lambda(v) - r$  crosses zero at  $v = \tilde{v}_B$ . Consequently, the term  $\lambda(v)/v$  can only contribute to the integral close to  $v \approx \tilde{v}_B$  (*i.e.*  $\tau \approx t$ ). Let us therefore expand the integrand as

$$\exp \left[ \tilde{v}_B \frac{\tilde{\lambda}(v)}{v} t + z \tilde{\lambda}'(v) \right] \simeq \exp \left[ \tilde{\lambda}'(\tilde{v}_B) (v - \tilde{v}_B) t + z \tilde{\lambda}'(v_B) \right]. \quad (\text{S48})$$

Performing the integral

$$\int_{\tilde{v}_B}^{\infty} \frac{dv}{v^2} \exp \left[ \tilde{\lambda}'(\tilde{v}_B) (v - \tilde{v}_B) t \right] = -\frac{1}{t} \frac{1}{\tilde{\lambda}'(\tilde{v}_B)}, \quad (\text{S49})$$

we obtain

$$\lim_{t \rightarrow \infty} \tilde{D}(t, x = \tilde{v}_B t + z) = \left( 1 - r \frac{\tilde{v}_B}{\tilde{\lambda}'(\tilde{v}_B)} \right) \exp \left[ z \tilde{\lambda}'(\tilde{v}_B) \right] \quad (\text{S50})$$

$$= \left( 1 + \frac{r}{\tilde{\lambda}_B} \right) \exp \left( -\frac{z}{\tilde{v}_B} \tilde{\lambda}_B \right), \quad (\text{S51})$$

where we introduced  $\tilde{\lambda}_B := -\tilde{v}_B \tilde{\lambda}'(\tilde{v}_B)$ . This concludes the proof of the existence of a wavefront traveling ballistically with an effective butterfly velocity  $\tilde{v}_B$  and with an effective Lyapunov rate  $\tilde{\lambda}_B$  as given by Eq. (S42) and (S43), respectively. In the particular case of a velocity-dependent Lyapunov of the form

$$\lambda(v) = \frac{\lambda_B}{\alpha} \left[ 1 - \left( \frac{v}{v_B} \right)^\alpha \right], \quad (\text{S52})$$

with  $\alpha \geq 1$ , this yields

$$\begin{cases} \tilde{v}_B = v_B \left( 1 - \frac{r}{\lambda_B} \right)^{1/\alpha} \\ \tilde{\lambda}_B = \lambda_B - r \end{cases} \quad \text{for } r < \lambda_B, \quad (\text{S53})$$

and  $\tilde{v}_B = \tilde{\lambda}_B = 0$  for  $r > \lambda_B$ .